Canadian Conference - Pacific Conference on Earthquake Engineering 2023

Vancouver, British Columbia

June 25th – June 30th, 2023

Optimization of fuzzy logic controller for high-tech machinery and building vibration

Chandrasekhara Tappiti[1], Tzu-Kang Lin[2]*

[1]PhD Scholar, Department of Civil Engineering, National Yang Ming Chiao Tung University, Taiwan
[2]Professor, Department of Civil Engineering, National Yang Ming Chiao Tung University, Taiwan
*tklin@nycu.edu.tw (Corresponding Author)

ABSTRACT

This paper presents the design of an optimal fuzzy logic control (FLC) algorithm for effectively attenuate microvibrations of a hybrid platform situated on the second floor of a building, which is exposed to ground motions induced by traffic. The hybrid platform serves as a protective measure to safeguard delicate equipment from vibrations caused by various sources such as traffic, machinery, and natural events like earthquakes, while it is positioned within the building structure. The FLC algorithm is employed to determine the suitable control force for active actuators, which is further enhanced through optimization using four evolutionary algorithms (EAs). These EAs are population-based metaheuristic algorithms inspired by nature: microgenetic algorithm (μ-GA), particle swarm optimization (PSO), differential evolutionary algorithm (DEA), and cuckoo search algorithm (CSA). The goal of optimization is to refine the FLC knowledge base and rule base. To demonstrate the effectiveness of the proposed method in controlling traffic-induced vibrations on a hybrid platform, a three-degree-of-freedom (3-DOF) structure, along with the platform, is considered. The evaluation of the hybrid platform control efficiency and its velocity level is performed based on the Bolt, Beranek, and Newman (BBN)-vibration criteria. The simulation results obtained using these innovative EAs show that the actively controlled platform successfully reduces the microvibration of a high-tech machinery. According to the findings, the PSO algorithm surpasses the other techniques in terms of velocity levels of the second floor and hybrid platform.

Keywords: microvibration control, high-tech machinery, evolutionary algorithms, BBN-vibration criteria, fuzzy logic controller.

INTRODUCTION

Generally, a significant concern in structural engineering and design is the control of vibration amplitudes, including operational and safety boundaries. One contemporary method for controlling vibration amplitude is based on the employing of structural control schemes, which fall into three primary groups: (1) passive, (2) active, and (3) hybrid control systems. Therefore, using these control schemes, it is vital to find the optimal controller for buildings under natural hazards [1] [2]. Among these protective systems, passive control systems reduce the impact of earthquake energy as the structure deform in accordance with the relative velocity or displacement of connection points. However, performance of passive systems is limited because they cannot be adjusted or tuned in accordance with changing external loads or structural features over time. These limitations can be addressed by using the active control systems, which are non-traditional approaches in structural engineering community [3]. Moreover, hybrid control systems are the improved devices of passive devices which will utilize both rate dependent and rate independent devices for the dissipation of seismic energy and reductions of the structural responses [4].

Modern buildings are designed to be spacious, slender, and versatile to support more vital functions. Structures with optimally positioned active and hybrid control systems are monitored and protected against natural hazard-induced vibrations through the careful design of control algorithms. However, these buildings typically cannot protect high-precision equipment from traffic-induced vibrations, which can cause moderate to severe equipment damage that is placed inside the building. High-tech machinery used to manufacture ultraprecision products must adhere to extremely strict vibration standards to work normally and to be protected against vibrations caused by both earthquake and traffic. These ground vibrations pose a serious threat to infrastructure and high-precision equipment, particularly in regions with high seismic activity or heavy traffic flow. However, Amiri and Bagheri [5] and Rofooei et al. [6] used wavelet analysis and nonstationary Kanai-Tajimi spectrum models to generate artificial acceleration time histories and traffic-induced ground motion. Various simulation experiments to derive nonstationary traffic driven ground motions have been performed [7] and have reported that traffic-induced ground motions have a dominant frequency range, which varies depending on the distance between the source and facility, the nearby soil conditions, and the type of the seismic waves. Therefore, the needs for microvibration control performance have become increasingly pressing as a result of the quick advancement of high-precision equipment in semiconductor industry, optical microscopes, and integrated circuits [8], [9]. Typically, equipment cost comprise 75% of the total capital expenditure for constructing a high-tech facility, whereas the amount spent on constructing building itself is less than 5% [10].

Pourzeynali, et al. [11] and Dounis, et al. [12] employed a genetic fuzzy logic controller (GFLC) approach to achieve active control for tall buildings with active tuned mass dampers in earthquake-prone regions in Iran. Their studies found that, GAs with FLC integration was effective for reducing the displacement response of the top floor. In addition to smart control of structures, it is essential to evaluate dynamic behavior and enhance the performance of structures with efficient control algorithms and well-known intelligent control techniques, thereby assessing the aspect of structures. Henceforth, Fisco and Adeli [13] [14] conducted a literature review study on control systems, control methodologies, and their practical implementation in smart structures with active, semi-active, and hybrid control. Marinaki, et al. [15] used a multi objective differential evolutionary algorithm to identify the best settings for a fuzzy controller that managed the vibration control of beams with piezoelectric sensors and actuators; their results for sinusoidal excitations are quite promising. Lin, et al. [16] introduced a novel GA-based design technique for viscous dampers in building structures that determined the optimal distribution of damping coefficients. According to the authors, the distribution of damping coefficient processes in each building story is not governed by codes, but it can be improved using their distribution methods. In later work, Azizi, et al. [17], [18] used the improved whale optimization algorithm, a hybrid optimization method called ant lion optimizer (ALO), and the Jaya algorithm to examine the performance of optimized fuzzy controllers for seismically excited tall buildings. Their numerical findings revealed that, response reductions are greater for 20-story buildings than the 3-story buildings. Xia, et al. [19] integrated a chaotic algorithm with optimal control theory to construct a fusion function to decrease the dimensionality of the fuzzy controller inputs for the double inverted pendulum problem, and their method performed well in simulations.

Henceforth, Azizi and Talatahari [20] proposed an arithmetic optimization algorithm (AOA), and improved upon AOA with fuzzy control membership functions and rule base in near-fault strong ground movement regions for nonlinear steel structures. The authors demonstrated that the improved method provides more competitive solutions than that of the standard AOA method, resulting in less structural responses and damage According to the literatures presented thus far, numerous researchers have acquired an interest in FLC theory due to its uncertainty, vigorous nonlinear performance, model-free controller, and good reliability in the field of vibration mitigation of civil structures as well as other scientific domains.

In general, semiconductor manufacturing industries and highly precious manufacturing firms may utilize the building floors or passive isolation systems to locate their high-tech facilities. Due to the lack of stiffness isolation devices and passive systems, it is difficult to control the vibrations of batch of high-tech machinery caused by near traffic induced ground motion. Furthermore, whereas many literatures are focusing and minimizing the structural responses to the natural hazards, but pay little attention to the vibrations of high precision equipment caused by traffic induced ground motions. As a result, it is essential to protect the high precision equipment in semiconductor industry from even micro-level vibrations, as these ae more expensive than the buildings themselves. To overcome these problems, hybrid control system which is composed of passive mounts and active actuators to mitigate the high-precision equipment vibrations under the traffic induced ground motions rather than the earthquake ground motions is investigated. In addition to these, the study developed an FLC for hybrid platform response mitigations, as it has a great capacity to deal with nonlinear problems using logical reasoning and as the majority of the literatures presented here use an FLC. Therefore, in this paper, optimal FLC has been studied as a consequence of EAs to optimize the fuzzy parameters and rule base for response mitigation of the hybrid platform vibration caused by the traffic-induced ground motion. Including that, this study intended to control microvibrations of a hybrid platform, in which ultraprecise equipment is placed and is subjected to traffic-induced ground motion rather than earthquake ground motion.

ANALYTICAL MODEL OF THE HYBRID PLATFORM

The performance of the designed hybrid control system was verified utilizing a three-story building structure with a hybrid platform on its second floor as shown in Fig. 1. The building and hybrid platform were stabilized using hybrid control (comprising active control and passive mounts with leaf springs). The passive control system is achieved with the incorporation of two leaf springs (Fig.1 (b)) on both sides of platform in a transverse direction (opposite to direction of traffic ground acceleration). In results of this, the leaf springs are pin supported between the building floor and platform to provide the additional horizontal stiffness of platform and to decrease the effect of axial force on elastic deformation of leaf springs. However, the active control system is achieved by utilizing the active actuators in the longitudinal direction. The equation of motion of the coupled building and hybrid platform system for the actively controlled platform shown in Fig. 1 can be expressed as follows:

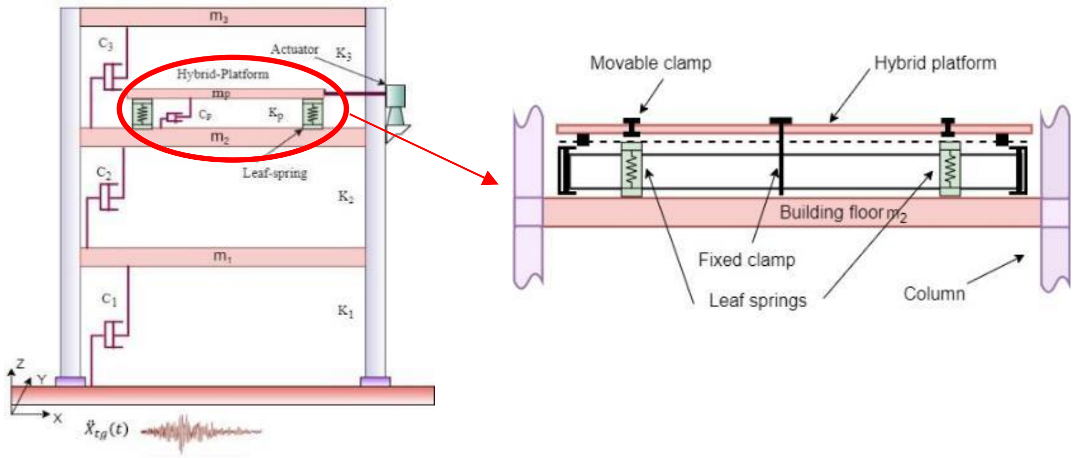

(a) Hybrid platform placed on a building floor *(a) hybrid platform cross-section in Y-direction positioned on leaf springs.*

Figure. 1. Configuration of model building and hybrid platform.

$$\begin{bmatrix} m_1 & 0 & 0 & 0 \\ 0 & m_2 & 0 & 0 \\ 0 & 0 & m_3 & 0 \\ 0 & 0 & 0 & m_p \end{bmatrix} \begin{Bmatrix} \ddot{x}_1 \\ \ddot{x}_2 \\ \ddot{x}_3 \\ \ddot{x}_p \end{Bmatrix} + \begin{bmatrix} c_{11} & c_{12} & c_{13} & 0 \\ c_{21} & c_{22}+c_p & c_{23} & -c_p \\ c_{31} & c_{32} & c_{33} & 0 \\ 0 & -c_p & 0 & c_p \end{bmatrix} \begin{Bmatrix} \dot{x}_1 \\ \dot{x}_2 \\ \dot{x}_3 \\ \dot{x}_p \end{Bmatrix} + \begin{bmatrix} k_{11} & k_{12} & k_{13} & 0 \\ k_{21} & k_{22}+k_p & k_{23} & -k_p \\ k_{31} & k_{32} & k_{33} & 0 \\ 0 & -k_p & 0 & k_p \end{bmatrix} \begin{Bmatrix} x_1 \\ x_2 \\ x_3 \\ x_p \end{Bmatrix} =$$

$$\begin{Bmatrix} 0 \\ -f_c \\ 0 \\ f_c \end{Bmatrix} + \begin{Bmatrix} c_{11}/2 \\ 0 \\ 0 \\ 0 \end{Bmatrix} \dot{x}_g + \begin{Bmatrix} k_{11}/2 \\ 0 \\ 0 \\ 0 \end{Bmatrix} x_g \tag{1}$$

where, m_i, k_i, c_i (i = 1, 2, 3) are the mass, stiffness coefficient, and damping coefficient of the ith floor (i = 1, 2, 3); x_i(i = 1, 2, 3) is the displacement of the ith floor; and x_g, $\dot{x}_g$, and $\ddot{x}_g$ are the displacement, velocity, and acceleration of traffic-induced ground motion, respectively. Similarly, m_p, k_p, and c_p are the mass, stiffness coefficient, and damping coefficient of the hybrid platform; x_p, $\dot{x}_p$, and $\ddot{x}_p$ are the displacement, velocity and acceleration of the hybrid platform; and f_c is the control force generated by the optimal FLC controller. The state-space equation of motion of the coupled building and hybrid platform system can be derived from Eq. 1 and is presented in Eq.2. By critiquing the state-space building model under the influence of traffic-induced ground motion, the uncontrolled second floor and hybrid platform response was generated.

$$\{\dot{z}\} = [A]\{z\} + \{B\}\, f_c + \{E_1\}\,\dot{x}_g + \{E_2\}\,x_g \tag{2}$$

where $\{z\} = \{x_1\ x_2\ x_3\ x_p\ \dot{x}_1\ \dot{x}_2\ \dot{x}_3\ \dot{x}_p\}^T$is the state vector of the coupled building and hybrid platform system, A is the system matrix, B is the control matrix, and E_1 and E_2 are the excitation matrixes, expressed as follows:

$$A = \begin{bmatrix} 0 & I \\ -M^{-1}K & -M^{-1}C \end{bmatrix},\ B = \begin{bmatrix} 0 \\ B_2\ M^{-1} \end{bmatrix},\ B_2 = \{0\ \ -1\ \ 0\ \ 1\}^T \tag{3}$$

$$E_1 = \{0\ 0\ 0\ c_{11}/2\ 0\ 0\ 0\ 0\}^T, E_2 = \{0\ 0\ 0\ k_{11}/2\ 0\ 0\ 0\ 0\}^T \tag{4}$$

where M, K, and C are the mass, stiffness coefficient, and damping coefficient matrixes, respectively, of the building and hybrid platform, and B_2 is the placement of the control force. The structural parameters of the building are as follows:

$$[\,M\,] = \begin{bmatrix} 100.7 & 0 & 0 \\ 0 & 100.7 & 0 \\ 0 & 0 & 91.8 \end{bmatrix} (kg) \tag{5}$$

$$[\,C\,] = \begin{bmatrix} 95.26 & -32.74 & 5.75 \\ -32.74 & 96.69 & -28.57 \\ 5.75 & -28.57 & 64.37 \end{bmatrix} (N\,s\,m^{-1}) \tag{6}$$

$$[\,K\,] = \begin{bmatrix} 3.5322 & -1.9364 & 0.2102 \\ -1.9364 & 3.4895 & -1.8079 \\ 0.2102 & -1.8079 & 1.6751 \end{bmatrix} \times 10^{6}\,(N\,m^{-1}). \tag{7}$$

The hybrid platform mass was set as 20.5 kg, which is 25% of the second-floor weight. The stiffness k_p, and damping coefficient c_p of platform were obtained as follows: $f_P = \left(k_p/m_p\right)^{1/2}/\,2\pi,\ \xi_p = c_p/\left(4\pi m_p k_p\right)$, where, f_P is the platform frequency and ξ_p is the damping ratio of the hybrid platform.

DESIGN OF OPTIMAL FUZZY LOGIC CONTROLLER

The established control algorithms for the mitigation of hybrid platform and second floor of the building vibration under traffic-induced ground motions depend on the control performance of smart control devices such as passive, active, and semi-active control. The FLC is a nonlinear control algorithm which can be utilized to assess the performance of control devices in earthquake engineering as well as other fields of engineering applications where structure responses are required to minimize. According to intelligence controllers, an FLC is better suited for problems involving nonlinearity and massive mathematical formations of input and output of physical systems. However, in cases involving problems with greater complexity and where response reductions are more important, it is necessary to optimize or tune the FLCs parameters and rule base. Consequently, the physical dynamic system may be more precisely tuned. An FLC structure yields the relative velocity and platform acceleration as inputs and provides control force as output. The input variables and output variable are normalized over the universe of discourse (UOD) of [-1, 1]. These inputs and output variables are mapped to their respective UOD using seven and nine MFs, of which the first and last MFs are S, Z-MFs, while middle MFs are chosen as gaussian MFs. The mapped MFs play a crucial role in FLC because they determine how a linguistic variable is mapped to a fuzzy set. Furthermore, these fuzzy sets represent the uncertainty and imprecision in the input and output variables, allowing the system to make decisions based on vague or incomplete information. The MFs variables for the fuzzy inputs and output are presented in Fig. 2. Moreover, the rule base is composed of 49 rules, with each input having seven MFs, and all of these rules are produced by using a geometric approach to update each rule set for every iteration.

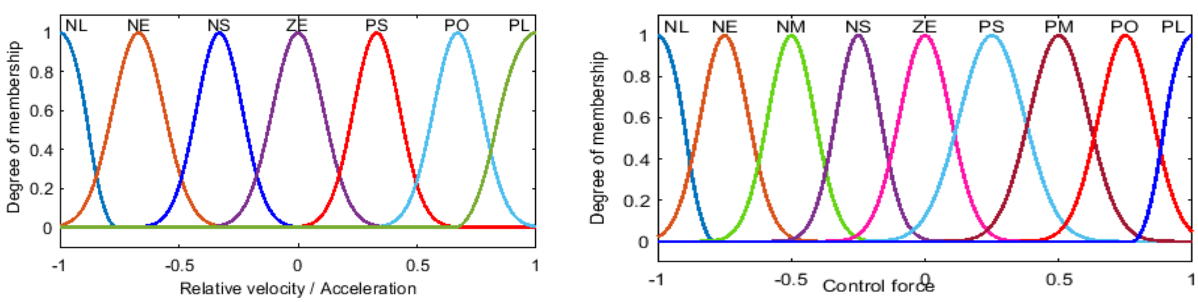

(a) *(b)*

Figure. 2. Optimization variables of membership functions (a) fuzzy inputs (b) fuzzy output.

The PSO, DEA, CSA, and μ-GA techniques are constructed to make possible to optimize the FLC variables utilizing the proposed strategy. As the EAs are robust and flexible heuristic search techniques based on the Darwinian evolution that capture global answers to many complex optimization problems in any field of research. These algorithms are having a higher probability of obtaining near optimal parameters or variables quickly than other techniques. The benefit of adopting these EAs is the ease with which the objective function can be selected, and can contain variables that are not state variables in control systems. Four of the following controllers were evaluated in the simulations; (i) FLC-PSO: FLC optimized using the PSO, (ii) FLC-DEA: FLC optimized by DEA, (iii) FLC-CSA: FLC optimized with CSA, and (iv) FLC-µ-GA: FLC optimized using the µ-GA are applied, and a comparative analysis is performed. Due to the limited number of pages, the comprehensive procedures for all four optimization algorithms are not provided at the present time. However, the pseudo code for optimizing a fuzzy controller using these four EAs is provided in Fig. 3.

While implementing the control algorithm for the microvibration control of hybrid platform, we assume that the building structure containing high-tech machinery is already protected against natural hazards. Furthermore, the main goal of the present study is to mitigate the hybrid platform velocity and displacement; thus, the objective functions were the ratios between the L_2 norm (Euclidian norm, selected to exponentially increase the influence of outliers) of the controlled and uncontrolled acceleration, velocity, and displacement responses of hybrid platform as defined in equation (8). These objective functions were combined into a single fitness function on the basis of weighted sum strategy and the equal weights are considered:

$$f_{obj} = \frac{\|\ddot{x}(t)\|}{\|\ddot{x}_{unc}(t)\|} + \frac{\|\dot{x}(t)\|}{\|\dot{x}_{unc}(t)\|} + \frac{\|x(t)\|}{\|x_{unc}(t)\|} \tag{8}$$

where, $\|\cdot\|$ is the L_2 norm of all state variables; $\ddot{x}(t)$, $\dot{x}(t)$, and $x(t)$ are the controlled acceleration, velocity, and displacement of the hybrid platform, respectively, and $\ddot{x}_{unc}(t)$, $\dot{x}_{unc}(t)$, and $x_{unc}(t)$ are the uncontrolled acceleration, velocity, and displacement of the hybrid platform, respectively.

- Step 1: Define the fuzzy logic controller with the desired input, output MFs and rule base.

- Step 2: Define the objective function that evaluates the performance of a FLC.

- Step 3: Initialize the population.

- Step 4: Evaluate the fitness of each member of population.

- Step 5: Repeat until convergence criteria satisfied.

- Step 6: Return the best solution.

- Step 7: Implement the optimized FLC to control the system.

Figure 3. Pseudo code for the optimization of fuzzy controller using the evolutionary algorithms.

NUMERICAL SIMULATION AND RESULTS

Numerical simulations are conducted for the three-story building model along with the hybrid platform, which is positioned on the second floor to suppress the response of high-precision equipment to ground motions induced by nearby traffic ground acceleration of PGA 0.05g. The traffic-induced ground accelerations are generated using the well-known and benchmark technique called a modified Kanai-Tajimi power spectrum (Eq. 9), which involves nonstationary characteristics as well as these ground motions are stochastic in nature.

$$S_{xx}^{KT}(\omega) = \frac{\left[1 + 4\ \xi_{g1}^2 (\omega/\omega_{g1})^2\right] (\omega/\omega_{g1})^2 U_0^2}{\left\{\left[1 - (\omega/\omega_{g1})^2\right]^2 + 4\,\xi_{g1}^2\ (\omega/\omega_{g1})^2\right\}} \times \frac{1}{\left\{\left[1 - (\omega/\omega_{g2})^2\right]^2 + 4\,\xi_{g2}^2\ (\omega/\omega_{g2})^2\right\}} \tag{9}$$

where ω_{g1}, ω_{g2}, ξ_{g1}, and ξ_{g2} are the parameters of ground motion and U_0 is ground acceleration intensity selected to mimic ground acceleration caused by traffic. The generated nonstationary traffic-induced ground acceleration is presented in Fig. 4. In practice, the high-tech machinery manufacturing buildings are well designed with sophisticated control techniques; nevertheless, the manufacturing platforms are may not be as adequately protected and while transporting from one place to other they are more vulnerable to microvibration of aforementioned ground accelerations. Therefore, the present study carries out with an independent assessment of lower PGA values rather than the earthquake ground motions. Furthermore, these ground accelerations are applying in either the X-direction or Y-directions independently. Because the velocity and displacement components were used as input excitations rather than applying acceleration in this study, the resulting acceleration time history is integrated twice to yield the displacement and velocity time histories. In order to eliminate velocity and displacement shifts, the acceleration time history is treated throughout the integration process using a high-band pass filter. The structural characteristics of the building and platform are given in equations (5) through (7) [8].

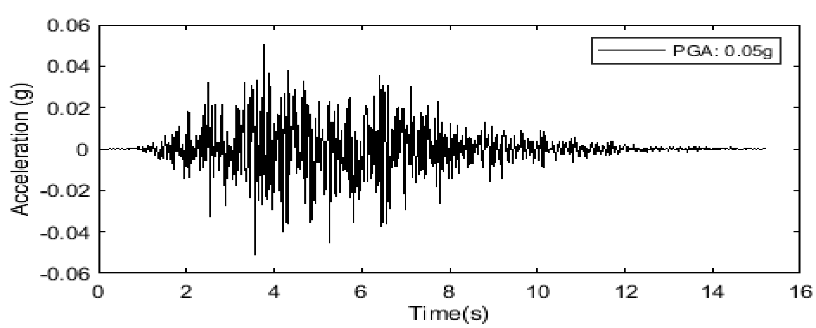

Figure 4. Input traffic-induced ground acceleration time history.

To demonstrated the feasibility of proposed EAs for hybrid platform and second floor of the building under traffic-induced vibrations, the optimized results with the PSO algorithm are compared with uncontrolled and traditional LQR controller. In Fig. 5, the forms of FLC-PSO algorithm, displacement and velocity response histories of the hybrid platform and second floor of the building structure are depicted. It is clear from the figure that the particle swarm algorithm successfully suppressed the displacement responses. When compared to the LQR controller, the velocity response of hybrid platform was not reduced significantly. Consequently, FLC-PSO algorithm is utilized to improve the velocity response reductions of hybrid platform. The absolute maximum displacement of hybrid platform is 0.808, 0.067, and 8.799×10^{-7} mm for uncontrolled, LQR, and FLC-PSO algorithm, respectively. While the comparable absolute displacement of the second floor for the uncontrolled, LQR, and FLC-PSO algorithm, respectively, is 0.984, 0.027, and 1.137×10^{-3} mm. At the same time, the velocity response of hybrid platform for the uncontrolled, LQR, and FLC-PSO algorithm is 68.53, 60.21, and 1.752 mm/sec, respectively. However, for the uncontrolled, LQR, and FLC-PSO controller, the comparable absolute velocity of second floor is 107.47, 59.23, and 23.09 mm/sec, respectively.

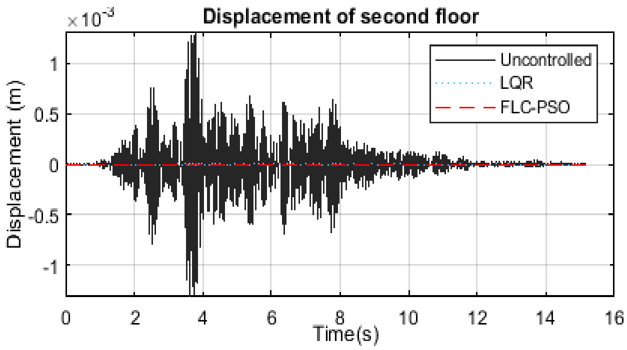

(a) Displacement history of the second floor

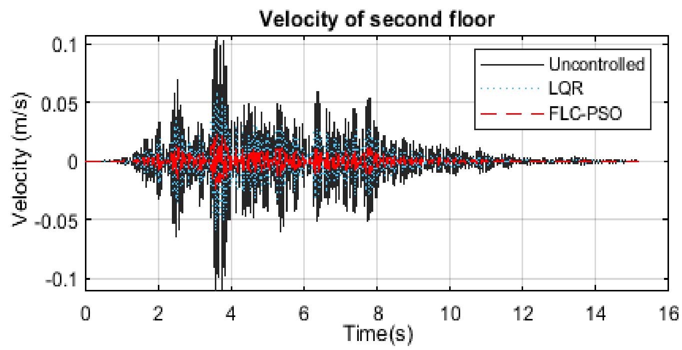

(b) Velocity history of the second floor

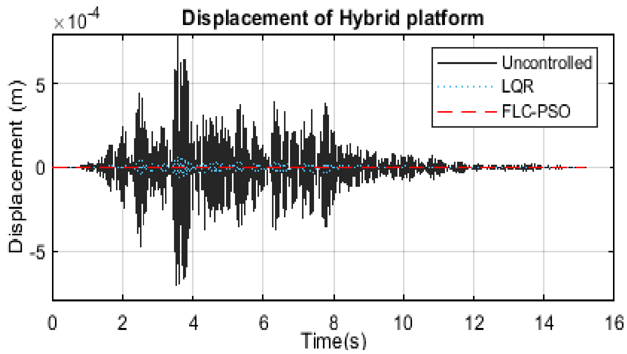

(c) Displacement history of hybrid platform

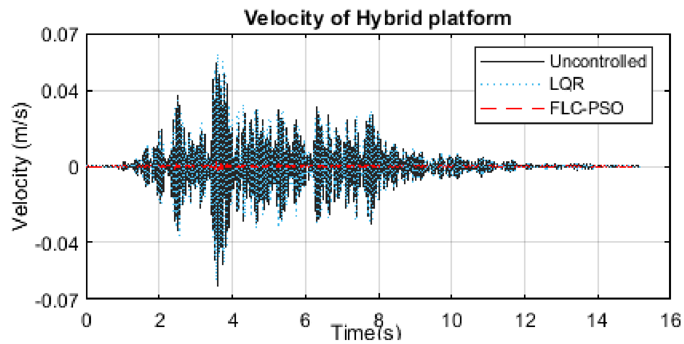

(d) Velocity history of hybrid platform

Figure 5. FLC-PSO algorithm time histories of second floor of the building and hybrid platform.

Similarly, the controlled displacement responses of a hybrid platform are1.218×10^{-6}, 1.303×10^{-6}, 1.353×10^{-6} mm for the DEA, CSA, and μ-GA algorithms. On the other hand, the displacement of the second floor are 1.117×10^{-3}, 1.346×10^{-3}, 1.396×10^{-3} mm for the same algorithms, respectively. In addition to the displacement responses, the controlled velocity response of the second floor for the optimal fuzzy controller with the DEA, CSA, and μ-GA algorithms are 26.65, 24.28, 29.61 mm/s, respectively. The controlled velocity response of the hybrid platform with the same optimization algorithms are 1.916, 1.971, and 2.026 mm/s, respectively. These displacement and velocity responses of the second floor and hybrid platform were contrasted with the various optimization algorithms listed in Tables 1 and 2. It is observed from these tables that PSO algorithm outrank the other algorithms, including the DEA, CSA, and μ-GA algorithms in response mitigation. For the active control of these composite hybrid platform and second floor responses, the PSO algorithm required 400 N of active control force. In addition to the uncontrolled and controlled time histories of the hybrid platform and second floor, the vibration levels of these systems are evaluated using the well-known BBN-vibration criteria. As the primary objective of this study is to attenuate the velocity levels of these systems and protect a high-tech machinery from the traffic-induced and floor-induced ground vibrations, the standard vibration criteria are taken into account.

Table 1. Comparison of absolute displacement of second floor of building and hybrid platform.

	Displacement comparisons with different optimization techniques (mm)					
	Unc	**LQR**	**FLC-PSO**	**FLC-DEA**	**FLC-CSA**	**FLC-μ-GA**
Second floor	0.984	0.027	1.137×10^{-3}	1.117×10^{-3}	1.346×10^{-3}	1.396×10^{-3}
	(1.00)	(0.027)	(1.155×10^{-3})	(1.135×10^{-3})	(1.367×10^{-3})	(1.418×10^{-3})
Hybrid	0.808	0.067	8.799×10^{-7}	1.218×10^{-6}	1.303×10^{-6}	1.353×10^{-6}
platform	(1.00)	(0.082)	(1.088×10^{-7})	(1.507×10^{-6})	(1.612×10^{-6})	(1.674×10^{-6})

Table 2. Comparison of absolute velocity of second floor of building and hybrid platform.

	Velocity comparisons with different optimization techniques (mm/sec)					
	Unc	**LQR**	**FLC-PSO**	**FLC-DEA**	**FLC-CSA**	**FLC-μ-GA**
Second floor	107.47	59.23	23.09	26.65	24.28	29.61
	(1.00)	(0.551)	(0.214)	(0.247)	(0.253)	(0.275)
Hybrid platform	68.53	60.21	1.752	1.916	1.971	2.026
	(1.00)	(0.878)	(0.025)	(0.028)	(0.0287)	(0.029)

Note: Numbers in parentheses represents the ratio between controlled to uncontrolled responses; Unc is a uncontrolled response.

Comparison of one-third octave band spectrum

The microvibration control performance for the hybrid platform was assessed using vibration criterion curves developed by the BBN-vibration criteria on the basis of velocity data regarding structural or fabrication devices at high-tech facilities before and after vibration issues were resolved. The simulation results, including the absolute velocity time histories of the hybrid platform and the second floor were converted to a one-third octave band spectrum (velocity spectrum). The velocity spectrum of the second floor in the absence of any control mechanisms was first examined to determine the if the location was suitable for the installation of high-precision equipment. Following that, as depicted in Fig. 6 (a), the velocity response spectrum of the second floor with the optimal FLC system, which is optimized by the PSO algorithm was then evaluated and compared with the BBN vibration criteria. According to the figure, the maximum velocity level of the second floor without any control measures was 72.12 dB with reference to 1 μ inch/sec. It is evidence that the velocity level violates the requirements for any kind of highly precise equipment. Therefore, it is necessary to attenuate the velocity levels of the second floor and the controlled level is 57.35 dB with the PSO algorithm. In Fig. 6 (b), the controlled and uncontrolled velocity spectrum of a hybrid platform was depicted; without a control mechanism the velocity level of a platform is 65.82 dB, which is more than what is required by the specifications. The controlled velocity level of a hybrid platform with the optimal fuzzy controller is 35.87 dB, it is less than those of the VC-E level. This shows that the hybrid-controlled platform is resilient in addition to having higher performance with the EA methods.

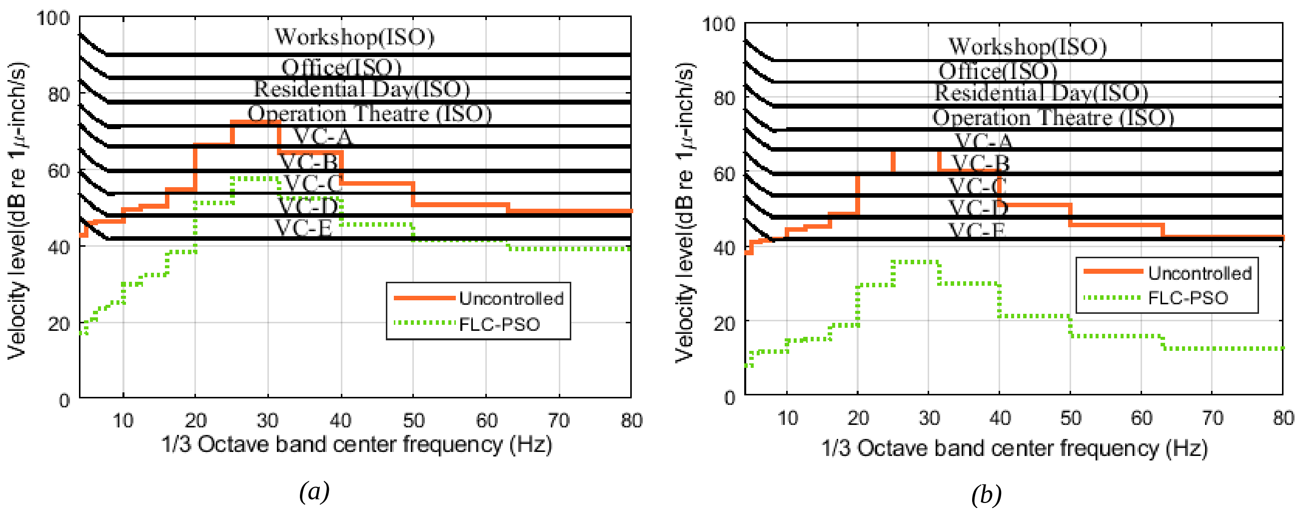

Figure 6. Uncontrolled and controlled velocity spectrum; (a) second floor velocity level, (b) hybrid platform velocity level.

CONCLUSION

An Fuzzy controller for reducing microvibration response to traffic-induced ground motions of a hybrid platform placed on the second floor of a building with nonlinear behavior was developed and optimized using the EAs. Due to the stochastic dynamic behavior of both high-tech facilities and building analysis, present study used the fuzzy controller because it is capable of handling complex, nonlinear and uncertain systems that are difficult to model mathematically. According to the simulation results, the displacement response of the hybrid platform and second floor of the building was reduced by approximately 99.0% for the EAs-based optimized FLC. The effectiveness microvibration control of the hybrid platform was also assessed using the BBN-vibration criteria. The one-third octave band velocity level of the hybrid platform, which is 35.87 dB, was less than the VC-E curve for the PSO algorithm and thus satisfies the most stringent BBN vibration criteria.

In addition to the mitigating the vibrations of high-tech machinery, the installation of the hybrid platform has no impact on building floor since it has been demonstrated significantly in the minimization of velocity and displacement response of the second-floor. Furthermore, the proposed controller is suggested for practical applications including the installation of hybrid platform for high-precision equipment in semiconductor industries. Consequently, experimental verification is essential for future studies to evaluate the potential of a hybrid platform with the optimal fuzzy controller to attenuate the microvibration of a high-tech machinery.

REFERENCES

[1] Spencer, B.F., and Nagarajaiah, S. (2003) State of the Art of Structural Control, *Journal of Structural Engineering.*, vol. 129, no. 7, pp. 845–856.

[2] Gaur, S., Elias, S., Höbbel, T., Matsagar, V.A., and Thiele, K. (2020) Tuned mass dampers in wind response control of wind turbine with soil-structure interaction, *Soil Dynamics and Earthquake. Engineering.*, vol. 132, pp.1-18.

[3] Fallah, N., and Ebrahimnejad, M. (2013) Active control of building structures using piezoelectric actuators, *Applied Soft Computing*, vol. 13, no. 1, pp. 449–461.

[4] Marshall, J.D., and Charney, F.A. (2010) A hybrid passive control device for steel structures, I: Development and analysis, *Journal of Constructional Steel Research*, vol. 66, no. 10, pp. 1278–1286.

[5] Amiri, G., and Bagheri, A. (2009) Simulation of earthquake records using combination of wavelet analysis and non-stationary Kanai-Tajimi model, *Structural Engineering and Mechanics*, vol. 33, no. 2, pp. 179–191.

[6] Rofooei, F.R., Mobarake, A., and Ahmadi, G. (2001) Generation of artificial earthquake records with a nonstationary Kanai-Tajimi model, *Engineering Structures*, vol. 23, pp. 827–837.

[7] Nelson, J.N. (1996) Recent developments in ground-borne noise and vibration control, *Journal of Sound Vibration*, vol. 193, no. 1, pp. 367–376.

[8] Yang, Z.C., Xu, Y.L., Chen, J., and Liu, H.J. (2003) Hybrid platform for vibration control of high-tech machinary in buildings subject to ground motion. Part 2: Analysis, *Earthquake Engineering and Structructural Dynamics*, vol. 32, no. 8, pp. 1201–1215.

[9] Xu, Y.L., Yang, Z.C., Chen, J., and Liu, H.J. (2003) Microvibration control platform for high technology facilities subject to traffic-induced ground motion, *Engineering Structures*, vol. 25, no. 8, pp. 1069–1082.

[10] Xu, Y.L., Liu, H.J., and Yang, Z.C. (2003) Hybrid platform for vibration control of high-tech machinary in buildings subjects to ground motion. Part 1: Experiment, *Earthquake Engineering and Structural Dynamics*, vol. 32, no. 8, pp.

[11] Pourzeynali, S., Lavasani, H.H., and Modarayi, A.H. (2007) Active control of high rise building structures using fuzzy logic and genetic algorithms, *Engineering Structures.*, vol. 29, no. 3, pp. 346–357.

[12] Dounis, A.I., Tiropanis, P., Syrcos, G.P., and Tseles, D. (2007) Evolutionary fuzzy logic control of base-isolated structures in response to earthquake activity, *Structural Control and Health Monitoring*, vol. 14, no. 1, pp. 62–82.

[13] Fisco, N.R., and Adeli, H. (2011) Smart structures: Part I - Active and semi-active control, *Scientia Iranica*, vol. 18, no. 3 A. Sharif University of Technology, pp. 275–284.

[14] Fisco, N.R., and Adeli, H. (2011) Smart structures: Part II - Hybrid control systems and control strategies, *Scientia Iranica*, vol. 18, no. 3 A. Sharif University of Technology, pp. 285–295.

[15] Marinaki, M., Marinakis, Y., and Stavroulakis, G.E. (2015) Fuzzy control optimized by a Multi-Objective Differential Evolution algorithm for vibration suppression of smart structures, *Computers and Structures.*, vol. 147, pp. 126–137.

[16] Lin, T.K., Hwang, J.S., and Chen, K.H. (2017) Optimal Distribution of Damping Coefficients for Viscous Dampers in Buildings, *International Journal of Structural Stability and Dynamics*, vol. 17, no. 4, pp. 1-19.

[17] Azizi, M., Ejlali, R.G., Mousavi Ghasemi, S.A., and Talatahari, S. (2019) Upgraded Whale Optimization Algorithm for fuzzy logic based vibration control of nonlinear steel structure, *Engineering Structures.*, vol. 192, pp. 53–70.

[18] Azizi, M., Ejlali, R.G., Mousavi Ghasemi, S.A., and Talatahari, S. (2020) Optimum design of fuzzy controller using hybrid ant lion optimizer and Jaya algorithm, *Artificial Intelligence Review*, vol. 53, no. 3, pp. 1553–1584.

[19] Xia, X., Xia, J., Gang, M., Zhang, Q., and Wang. (2020) Discrete Dynamics-Based Parameter Analysis and Optimization of Fuzzy Controller for Inverted Pendulum Systems Based on Chaos Algorithm, *Discrete Dynamics in Nature and Socity*, vol. 2020, pp. 1-8.

[20] Azizi, M and Talatahari, S. (2022) Improved arithmetic optimization algorithm for design optimization of fuzzy controllers in steel building structures with nonlinear behavior considering near fault ground motion effects, *Artificial Intelligence Review*, vol. 55, no. 5, pp. 4041–4075.